# Oxyhalogen−Sulfur Chemistry: Kinetics and Mechanism of Oxidation of Amidinothiourea by Acidified Iodate[1]

**Edward Chikwana and Reuben H. Simoyi***

*Department of Chemistry, Portland State University, Portland, Oregon 97207-0751*

*Received: September 10, 2003; In Final Form: November 2, 2003*

The oxidation of guanylthiourea, GTU, by mildly acidic iodate and molecular iodine has been studied. Its reaction with iodate shows an oligooscillatory formation and consumption of iodine in batch conditions. The major oxidation product is a ring-cyclized product of guanylthiourea, 3,5-diamino-1,2,4-thiadiazole (GTU-C), in which the thioureado moiety is oxidized to the unstable sulfenic acid that instantly attacks the distal amino group, eliminating water and forming the five-membered thiadiazole group. In excess GTU conditions, the stoichiometry of the reaction was 1:3 without any further oxidation past a 2-electron transfer, $IO_3^- + 3H_2NC(=NH)NH(C=S)NH_2 \rightarrow I^- + 3GTU\text{-}C + 3H_2O$, whereas in excess iodate conditions the stoichiometry is $2IO_3^- + 5H_2NC(=NH)NH(C=S)NH_2 + 2H^+ \rightarrow 5GTU\text{-}C + I_2(aq) + 6H_2O$. In high acid environments the reaction shows two peaks in iodine concentrations in batch conditions, and at lower acid concentrations one observes an induction period followed by a monotonic formation of iodine according to the Dushman reaction. The overall reaction is heavily catalyzed by iodide. The direct reaction of iodine and GTU is fast, with a bimolecular rate constant of $(1.10 \pm 0.20) \times 10^4\ M^{-1}\ s^{-1}$. This reaction is autoinhibitory with the product, iodide, inhibiting the reaction by forming the relatively inert $I_3^-$ species. Acid also inhibits the oxidation of GTU by iodine by protonating the thiol group, thereby reducing its nucleophilicity. A simple mechanistic scheme comprising 9 elementary and composite reactions was found to be adequate in explaining the full reaction scheme.

## Introduction

Thiols and thiocarbamides, in general, are very important physiological molecules. Thiourea and its derivatives form a vast group of highly reactive and physiologically active compounds.[2] In general, the substituted thioureas are toxic.[3] Animal studies on the toxicity of thiourea have shown that when it is administered in drinking water it induces thyroid adenomas and carcinomas in rats.[4] No one knows the origin of tumorigenicity in this series of compounds, but speculation is that these physiological effects can be rationalized from their reactivities.[5] Most studies on the effect of thioureas on human health have been reported without any mechanistic rationalization of these effects.

We recently embarked on a series of experiments aimed at rationalizing observed physiological effects of several organosulfur compounds on the basis of their reactivities.[6] Thiols are strongly implicated as antioxidants in human health although the mechanistic basis for such assertions has never been established.[7] Antioxidants are needed to prevent the formation of and oppose the actions of reactive oxygen species which are generated in vivo and cause damage to DNA, lipids and proteins. All indications are that metabolic processes of all organic sulfur compounds are oxidative.[8] This is a reasonable assumption. Sulfur in most organic compounds is nucleophilic, and these centers are susceptible to metabolic oxidation, especially S-oxygenation in which a series of successive sulfur oxo-acids are formed.[9] These sulfur oxo-acids, sulfenic, sulfinic and sulfonic acids, are physiologically active, and most physiological effects of the parent compounds can be ascribed to their formations. For example, the teratogen thioacetamide's physiological effects can be traced to the formation of the *S*,*S*-dioxide formed during the metabolism of thioacetamide.[10] Most of the oxidative processes, physiologically, are aided by standard enzymatic systems such as the P-450 groups and the flavin-containing monooxygenases.[11,12] These enzymatic systems, however, cannot aid a reaction that is not intrinsically feasible.

S-Oxygenation studies have proved to be very useful in predicting the toxicities of several thiocarbamides. Very similar thiols and thiocarbamides can physiologically express vastly varying degrees of toxicities. For example, though phenylthiourea is extremely toxic to rats, surprisingly, diphenylthiourea is innocuous.[13−15] The metabolites of phenylthiourea include inorganic sulfate and an organic urea residue, and those of diphenylthiourea are ring-cyclized metabolites with an intact thione group.[13] This has led to the general conjecture that, maybe, the degree of desulfurization can be related to the attendant toxicity.[16] Bolstering this assertion has been a series of experiments that show that the cleavage of a C−S bond can initiate the formation of reactive oxygen species from the initial generation of the sulfoxyl anion-radical which is derived from the cleavage of this bond.[17]

Guanylthiourea, GTU, is an extremely important industrial and biological molecule. In conjuction with mercaptobenzo-

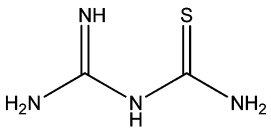

guanylthiourea

thiazyl disulfide, it is used as an accelerator in sulfur vulcanization of natural rubber. In inorganic synthesis its special structure has been used to synthesize anion-caged supermolecular compounds. It is in the field of medicine that it has been found to

10.1021/jp0367068 CCC: $27.50 
Published on Web 01/17/2004

be extremely important. It is a well-known stimulator of intestinal peristalsis and has been experimentally used for the clinical treatment of bowel paresis in peritonitis.[18] It has also been very promising in clinical trials as an immunostimulant and tumor cell inhibitor.[19,20] Generally, compounds incorporating the thioureido and guanidino structures, as GTU, are useful as radioprotective agents.[21] GTU and its derivatives gave a 66% survival rate in lethal radiation doses.

Very few studies had been performed on the oxidation mechanisms of GTU. A few studies had addressed the reaction of GTU with hydrogen peroxide but not on a mechanistic basis. We believe most of these varied metabolic effects expressed by GTU are derived from its oxidative metabolites. If we can evaluate its oxidation mechanism, we may also be able to predict and match substituted GTU's with their physiological effects. Our previous studies on oxyhalogen−sulfur chemistry had clearly indicated that the metabolic route through the sulfur oxo-acids was dominant.[22] We chose the oxidants acidic iodate and iodine because of their mildness and the fact that the reaction of the thiocarbamide moiety with molecular iodine has been implicated as the most important process in the goitrogenic effects of many thiocarbamides.[4]

## Experimental Section

**Reagents.** Doubly distilled water was used for preparation of all stock solutions. The following reagents were used without further purification: guanylthiourea, GTU, 97% (Acros), potassium iodate (Aldrich), potassium iodide, sodium perchlorate, and perchloric acid (70%) (Fisher). Iodine (Aldrich), was used as the resublimed 99.8% crystalline solid. A saturated solution of iodine was prepared by adding an excess amount of iodine crystals and stirring for a 24 h period and then letting the resulting solution to settle overnight. A clear, saturated solution was obtained and standardized against thiosulfate with starch as the indicator. Iodine concentrations were also determined spectrophotometrically by measuring the iodine absorbance at 460 nm, which was the experimentally determined isosbestic point. The absorptivity coefficient was found to be 770 $M^{-1}$ $cm^{-1}$. It is difficult to dissolve iodine concentrations past $10^{-3}$ M; however, the solubility was greatly enhanced by the use of potassium iodide. Higher aqueous iodine concentrations could be prepared by using excess potassium iodide concentrations or carefully measured ratios of iodine to KI. The stock solutions of GTU were prepared fresh daily and protected from light by covering with aluminum foil.

**Methods.** Reactions were run at a constant ionic strength of 1.0 M by adding the required amount of sodium perchlorate. Reaction temperature was maintained at 25 ± 0.1 °C. The two reaction systems studied, $IO_3^-$−GTU and $I_2$−GTU reactions, were found to be too fast for conventional methods; thus all kinetic studies were performed on a Hi-Tech Scientific Double-Mixing SF61-DX2 stopped-flow spectrophotometer. Digitization and amplifying was done via an Omega Engineering DAS-50/1 16-bit A/D board interfaced to a Pentium II 450 MHz computer. Potassium iodate, perchloric acid, and sodium perchlorate were premixed in one vessel at double the reactor concentrations as one of the reagent solutions, with the other solution containing only GTU.

**Stoichiometric Determinations.** Stoichiometric determination of the iodate−GTU reaction was performed both in excess $IO_3^-$ and in excess GTU. In the former case the total oxidizing power of ($IO_3^-$ + HOI + $I_2$) was determined by titration. Excess acidified iodide was added to the reaction solution, and the released iodine was titrated against standard thiosulfate Sulfate could be qualitatively tested by $BaCl_2$. Iodine formed in excess $IO_3^-$ was also determined separately by its absorbance at 460 nm ($\epsilon$ = 770 $M^{-1}$ $cm^{-1}$). The stoichiometry of the direct $I_2$−GTU reaction was determined spectrophotometrically and by titration. Standardized iodine solution was titrated from a buret into a GTU solution of known strength. The end point of the titration could be detected as the point where the iodine color lingers. This end point could also be enhanced by starch indicator.

## Results

**Stoichiometry.** The stoichiometry of the reaction was 1:3 with no variations: 1 mol of $IO_3^-$ to 3 mol of GTU. This would suggest a 2-electron oxidation of the sulfur center in GTU (the most nucleophilic part of the molecule). Such an oxidation would give the well-known unstable sulfur oxo-acid: sulfenic acid. Without adequate steric factors, we do not expect the sulfenic acid to be stable.

$$IO_3^- + 3H_2NC(=NH)NH(C=S)NH_2 \rightarrow I^- + 3H_2NC(=NH)NHC(=NH)CSOH \quad (R1)$$

The sulfenic acid will either dimerize (in the presence of excess GTU)

$$H_2NC(=NH)NH(C=S)NH_2 + H_2NC(=NH)NHC(=NH)CSOH \rightarrow (H_2NC(=NH)NHC(=NH)CS-)_2 + H_2O \quad (R2)$$

or disproportionate to the more stable sulfinic acid:

$$2H_2NC(=NH)NHC(=NH)CSOH \rightarrow H_2NC(=NH)NHC(=NH)CSO_2H + H_2NC(=NH)NH(C=S)NH_2 \quad (R3)$$

However, because there was no evidence for any further oxidation past the 2-electron transfer, reaction R3 could not be justified. Upon running the products through a GC−mass spectrometer, a number of fragments were observed, with one corresponding to the dimeric species formed in reaction R2, above, and a strong predominant peak for a product with a molecular weight of 116.4. This is the ring-cyclized product; 3,5-diamino-1,2,4-thiadiazole (GTU-C) with the structure:

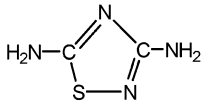


We conclude that the stoichiometry of the reaction in excess GTU is

$$IO_3^- + 3H_2NC(=NH)NH(C=S)NH_2 \rightarrow I^- + 3GTU\text{-}C + 3H_2O \quad (R4)$$

Excess iodate conditions produced molecular iodine as a product. The amount of iodine produced was 0.2 times the amount of GTU used. This was proved spectrophotometrically and was highly reproducible (see Figure 3a). The oxidizing power of the reaction solution, using iodometric techniques, however, did not vary from that obtained from stoichiometry R4. In excess iodate, this power was distributed into the different iodine species: iodine, iodate, and the other oxy-iodine species. This led to the deduction that excess iodate conditions involved the

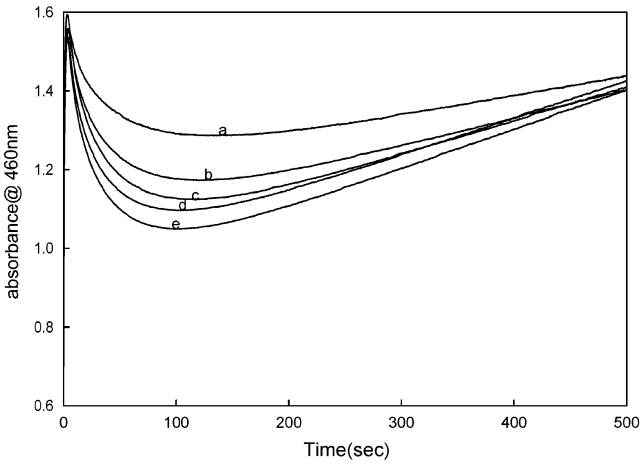


**Figure 1.** Effect of progressively increasing $[IO_3^-]$ at constant acid and [GTU]. Oligooscillations in iodine concentrations are observed. Final iodine concentrations in all traces shown are the same. $[GTU]_o = 0.01$ M, $[H^+] = 0.05$ M, $[IO_3^-]_o =$ (a) 0.01, (b) 0.02, (c) 0.03, (d) 0.04, (e) 0.05 M.

addition of the Dushman reaction[23−25] to reaction R4; eliminating $I^-$:

$$IO_3^- + 5I^- + 6H^+ \rightarrow 3I_2 + 3H_2O \qquad (R5)$$

Addition of 5R4 + R5 gives the observed stoichiometry in excess iodate conditions with the 5:1 ratio of substrate to iodine formed:

$$2IO_3^- + 5H_2NC(=NH)NH(C=S)NH_2 + 2H^+ \rightarrow 5GTU\text{-}C + I_2(aq) + 6H_2O \quad (R6)$$

**Reaction Dynamics.** The reaction is very complex and oligooscillatory in molecular iodine. Figure 1 shows a series of typical absorbance traces collected at 460 nm to follow the production of molecular iodine. In these highly acidic conditions there is an initial rapid formation of iodine followed by its consumption. All traces shown in Figure 1 were at excess iodate environments (i.e., ratio $[IO_3^-]_0/[GTU]_0 > 0.33$), and so the final stoichiometry would be R6 with iodine as one of the products. Thus, after this transient consumption of iodine, there is a final iodine formation that will ultimately give stoichiometry R6. Because the initial substrate concentration, $[GTU]_0$, is fixed, all traces shown in Figure 1 will finally give the same concentration of iodine, which in this series of experiments, was 0.002 M with an absorbance of approximately 1.55. Surprisingly, higher iodate concentrations supported a much more rapid rate of transient iodine consumption (see trend in traces a−e in Figure 1, ca. 100 s). (This would be unexpected if it is assumed that the Dushman reaction (R5) is wholly responsible for the formation of iodine.)

Figure 2a shows a closer examination of the initial stages of the data shown in Figure 1. Remarkably, one sees a series of highly reproducible traces with an initial well-defined induction period followed by a rapid formation of iodine. The induction period, at pH 2 and below is only a few seconds in duration. Iodate concentrations, as shown in Figure 2a, appear to control not only the induction period but also the rate of formation of iodine after the induction period. One can assume that the end of the induction period represents the point at which the reactions forming iodine (e.g., (R5)) supersede those that consume it. In a sense, the induction period can be used to

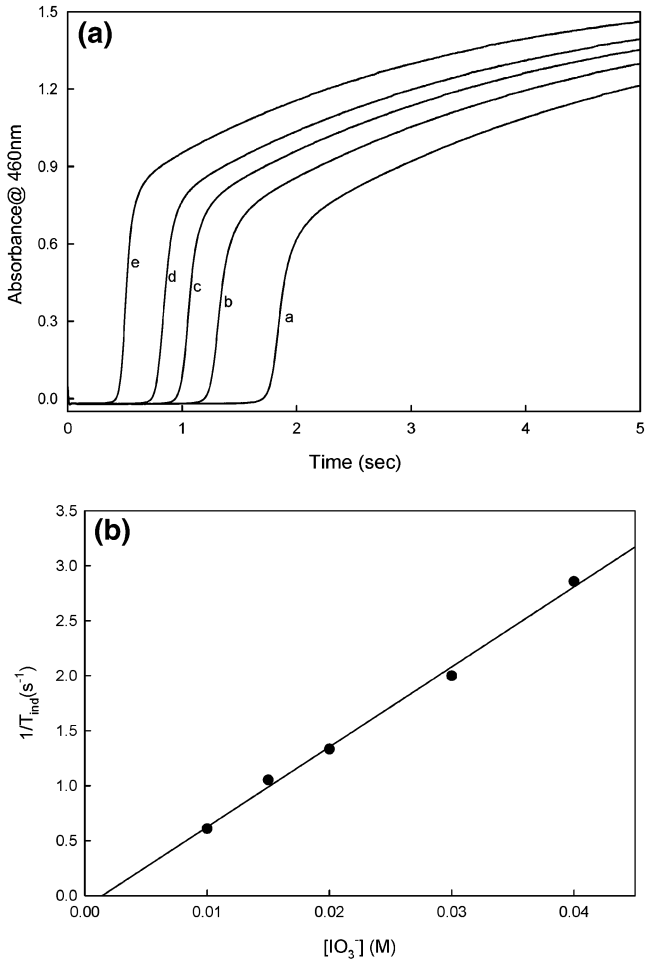


**Figure 2.** (a) Effect of $[IO_3^-]$ variation on its oxidation of GTU for the initial part of the reaction showing a finite and measurable induction period before formation of iodine. $[GTU]_o = 0.01$ M, $[H^+]_o = 0.02$ M, $[IO_3^-]_o =$ (a) 0.01, (b) 0.015, (c) 0.02, (d) 0.03, (e) 0.04 M. (b) Linear plot of reciprocal induction time vs $[IO_3^-]_o$ for data shown in Figure 2a.

estimate the rate of reaction because the inverse of the induction period should be proportional to the rate of reaction. A plot of the inverse of the induction time versus initial iodate concentration gives a straight line (Figure 2b). This indicates that the rate-determining step is dependent on iodate concentrations to the first power. The plot in Figure 2b can also be used to evaluate stoichiometry R4. For as long as GTU is in stoichiometric excess, no iodine will be formed, and stoichiometry R4 will dominate. These conditions will not produce iodine at low acid concentrations, and the induction period will approach infinity with the inverse of this value being zero. As soon as iodate is in excess, a finite induction time is observed. Figure 2b confirms this stoichiometry by delivering an intercept for infinite induction time, which gives a limiting stoichiometric ratio of 1:3 before iodine formation.

Acid merely acts as a very powerful catalyst in the oxidation of GTU. Figure 3a shows that although acid reduces the induction period, it does not influence anything else. All traces shown in this figure, as expected, end up delivering the same amount of molecular iodine, which is controlled (at excess iodate concentrations) by the amount of GTU available. With $[GTU]_0 = 0.01$ M, we expect 0.002 M iodine with a final absorbance of approximately 1.55, as shown in Figure 3a. A plot of induction period versus the inverse of the square of the acid concentrations shows a straight line, indicating that the reaction

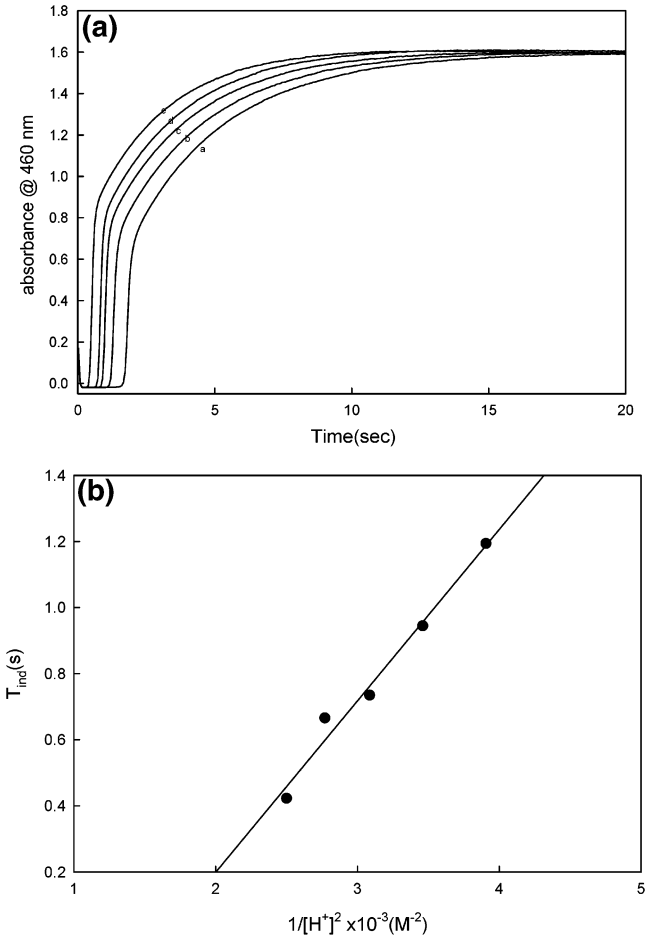


**Figure 3.** (a) Effect of varying acid concentrations for reactions run in excess iodate. Acid is not a reactant in the reaction but strongly catalyzes the reaction by reducing the induction period. $[GTU]_o = 0.01$ M, $[IO_3^-]_o = 0.03$ M, $[H^+]_o =$ (a) 0.015, (b) 0.016, (c) 0.017, (d) 0.018, (e) 0.02 M. (b) Plot showing the linear dependence of induction time on the reciprocal of $[H^+]^2$. $[GTU]_o = 0.01$ M, $[IO_3^-]_o = 0.03$ M. The plot is derived from data shown in Figure 3a.

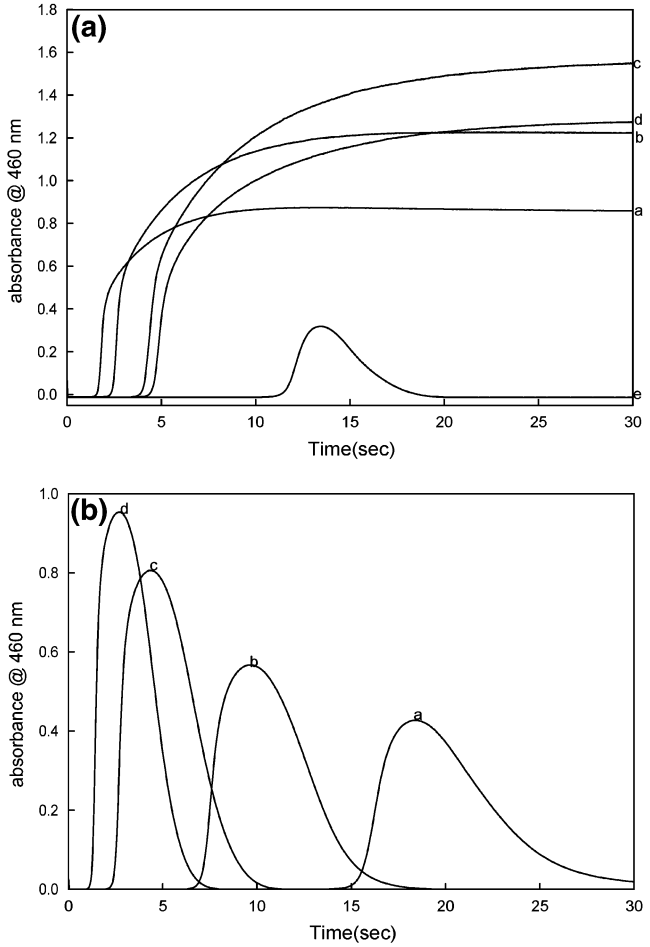


**Figure 4.** Absorbance traces for GTU variation in its oxidation by iodate. Initially, the absorbance increased (a)−(c) and as the stoichiometric point (e) is approached they start to decrease (c)−(e). There is also a direct relationship between the induction period and GTU concentration as expected. $[IO_3^-]_o = 0.005$ M, $[H^+]_o = 0.02$ M, $[GTU]_o =$ (a) 0.005, (b) 0.0075, (c) 0.01, (d) 0.0125, (e) 0.015 M. (b) Effect of acid variation at stoichiometric point (trace (e) from Figure 4a). The effect of acid can be seen in the form of a shorter induction period and a higher maximum iodine concentration. $[GTU]_o = 0.015$ M, $[IO_3^-]_o = 0.005$ M, $[H^+]_o =$ (a) 0.02, (b) 0.022, (c) 0.026, (d) 0.03 M.

responsible for the formation of iodine is dependent on acid to the second power (see Figure 3b).

**Iodate:GTU Ratios.** The most important parameter in determining reaction dynamics is the oxidant-to-reductant ratio, $R = [IO_3^-]_0/[GTU]_0$. At fixed acid concentrations, a variation of $R$ will show successively, as $R$ is reduced, an induction period with a monotonic formation of iodine, an induction period with two peaks in iodine concentrations (see Figure 1), an induction period with transient formation of iodine (Figure 4a, trace e), and no iodine formation at all (at very low $R$ values). Traces a−d in Figure 4a represent excess iodate concentrations with $R > 0.333$. Trace e represents the stoichiometric equivalent with $R = 0.333$. Yet, remarkably, it shows transient formation of iodine even though stoichiometry R4 does not support iodine formation. Such oligooscillatory behavior[26,27] can only be supported by the existence of nonlinear kinetics, most likely fueled by autocatalysis in one of the reactions involved in the reaction network. Taking trace e in Figure 4a and varying acid at this stoichiometric ratio gives the traces shown in Figure 4b. High acid concentrations give shorter induction periods, higher transient iodine concentrations, and higher rates of depletion of iodine as the reaction heads toward stoichiometry R4. Eventually, as acid is continuously reduced, no transient formation of iodine is observed, and the reaction monotonically attains stoichiometry R4.

**Direct Reaction of Iodine and GTU.** Apart from the Dushman reaction,[28] the direct oxidation of GTU by iodine is the most important reaction in this mechanism. The rate of this oxidation will determine whether GTU and iodine can coexist at the time scales of the GTU−$IO_3^-$ reaction. If the $I_2$−GTU reaction is fast, then formation of iodine would denote that all the GTU has been consumed. Figure 5a shows that the rate of this reaction is comparable to the iodate−GTU reaction. The remarkable feature of the iodine−GTU reaction is that it starts off extremely rapidly but quickly slows itself down about 0.5 s into the reaction. It would appear that it is autoinhibitory. The only product of the reduction of iodine is iodide. Addition of iodide is shown, in Figure 5b, to be inhibitory (as expected). To enhance the solubility of iodine, each reaction solution shown in Figure 5b was prepared as an equimolar mixture if $I_2/I^-$. For example, carefully weighed out crystals of iodine were added to a 0.001 M KI solution for trace a. In this case, the mixture of 0.001 M each of $I_2$ and $I^-$ gave a final species distribution of $[I_2] = [I^-] = 3.36 \times 10^{-4}$ M and $[I_3^-] = 6.64 \times 10^{-4}$ M. The five traces shown are not very different from each other due to the fact that, in all cases, there is enough iodide, such

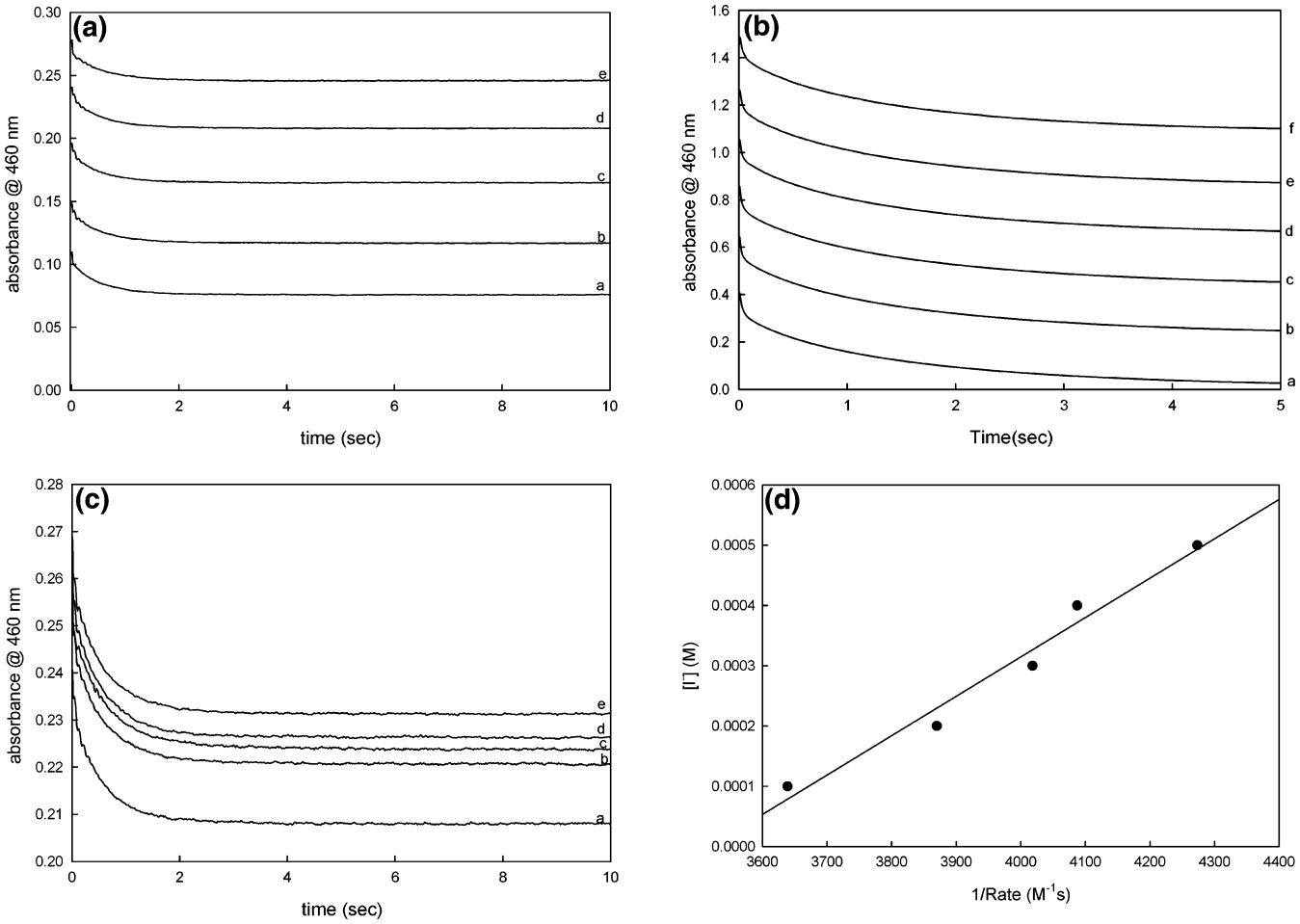


**Figure 5.** (a) Varying iodine concentrations for condition of excess iodine. (Iodine solutions were prepared by dissolving iodine crystals in water, and no iodide was added to enhance solubility.) The reaction is initially very fast but is essentially over within a second in these unbuffered reaction conditions. $[GTU]_o = 0.0001$ M, $[I_2]_o =$ (a) $2.8 \times 10^{-4}$ M, (b) $3.4 \times 10^{-4}$ M, (c) $3.9 \times 10^{-4}$ M, (d) $4.5 \times 10^{-4}$ M, (e) $5.0 \times 10^{-4}$ M. (b) Absorbance traces of the reaction between GTU and $I_2/I_3^-$ showing the effect of progressively increasing iodine concentration. Equimolar iodine−iodide concentrations were used to enhance solubility of iodine. These series of reactions are considerably slower than those in Figure 5a without added iodide. The reaction starts nearly as fast as the experiments in Figure 5a but quickly decelerates as more iodide is formed. $[GTU]_o = 0.001$ M, $[I_2]_o =$ (a) 0.001, (b) 0.00125, (c) 0.0015, (d) 0.00175, (e) 0.002, (f) 0.0025 M. (c) Effect of iodide variation on the oxidation of GTU by iodine for trace d in Figure 5a. There is a decrease in the initial rate of reaction as iodide concentration is increased and the reaction takes much longer to go to completion $[GTU]_o = 0.0001$ M, $[I_2]_o = 4.5 \times 10^{-4}$ M; $[I^-]_o =$ (a) no iodide, (b) $2.0 \times 10^{-4}$ M, (c) $3.0 \times 10^{-4}$ M, (d) $4.0 \times 10^{-4}$ M, (e) $5.0 \times 10^{-4}$ M. (d) Plot of inverse of reaction rate vs iodide concentrations for the data shown in Figure 5c. The plot is based on eq 3 where the intercept is $-K_{eq}^{-1}$ and the slope will allow for the evaluation of $k_{13}$. This plot gives $K_{eq} = 440 \pm 40$ M with a $k_{13} = (1.10 \pm 0.2) \times 10^4$ $M^{-1}$ $s^{-1}$.

that most of the iodine used as oxidant is converted, predominantly, to triiodide:[29]

$$I_2(aq) + I^- \rightleftharpoons I_3^-(aq) \qquad K_{eq} = 770\ M^{-1} \qquad (R7)$$

Despite this, a discernible inhibition is still observed with iodide. The inhibition is due to the different reactivities of $I_2$ and $I_3^-$.

Figure 6a shows the inhibitory effect of acid on the direct reaction of iodine with GTU. Within a small range of acid concentrations, pH 2−3, there is an inverse dependence of the initial rate of iodine consumption with acid (see Figure 6b). Figure 7 shows how rapidly the reaction commences before it autoinhibits. The traces shown are at different GTU concentrations and fixed $[I_2]_0$. One expects the initial absorbance observed at 460 nm to be approximately 1.16 for all traces. The trace with the lowest GTU concentration gives the expected initial absorbance due to iodine, but the rest give initial absorbances that are much less than 1.16. This means, then, that, within the mixing and "dead time" of our stopped-flow instrument, more than half of the reaction will have occurred in traces c−e.

**Catalytic Effect of Iodide.** Results from the direct reaction of iodine and GTU show an autoinhibitory effect from iodide (Figure 5b). Investigations were made into the effect of iodide ions on the whole reaction (Figure 8). Trace a with no iodide added (apart from that initially available in iodate solutions) has a longer induction period before formation of iodine. Addition of more iodide progressively decreased the induction period. Addition of iodide also increased the final amount of iodine obtained (in excess iodate conditions). This is to be expected if the Dushman reaction[28] is a major player in this mechanism.

## Mechanism

The reaction dynamics suggest that the standard oxyiodine reactions are dominant in this mechanism. The dependence of the reaction rate on the acid concentrations to the second-order implicate the well-known first step in the reduction of iodate:[24]

$$IO_3^- + 2H^+ + 2e^- \rightarrow HIO_2 + OH^- \qquad (R8)$$

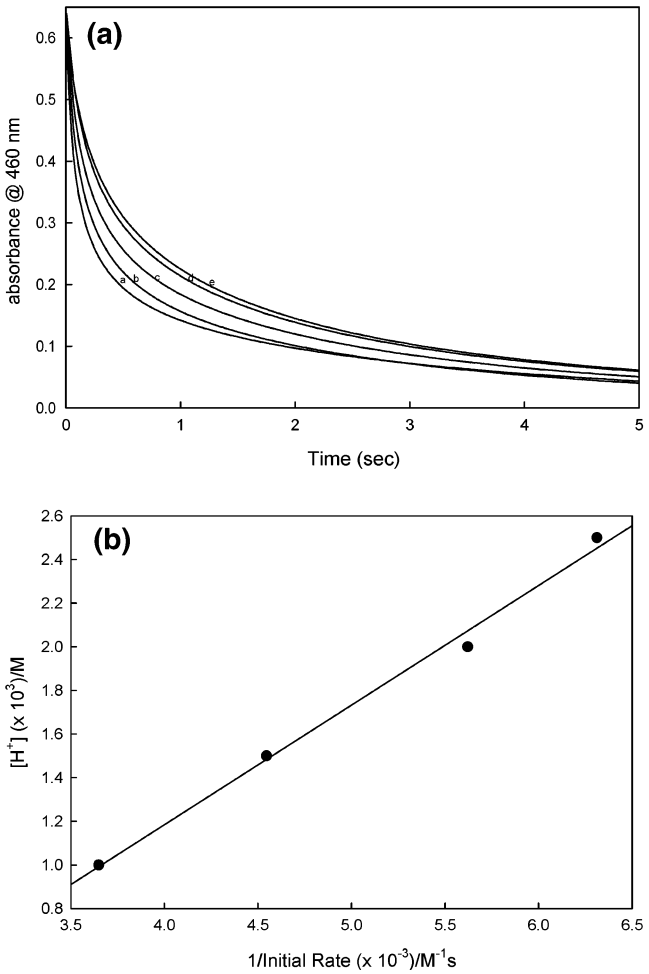


**Figure 6.** (a) Effect of varying acid concentration on the reaction of GTU and iodine. The iodine used here is dissolved in equimolar solutions with iodide. The initial rate of reaction decreases as the acid concentration is increased. $[GTU]_o = 0.001$ M, $[I_2]_o = 0.001$ M, $[H^+]_o$ = (a) 0.001, (b) 0.0015, (c) 0.002, (d) 0.0025, (e) 0.003 M. (b) Inverse acid dependence plot of the initial rate of the $I_2-GTU$ reaction for data shown in Figure 6a. This is the same plot as the one shown in Figure 5d with the intercept giving $K_a^{-1}$.

The two electrons can be supplied by any 2-electron reductant. This initial step has been extensively studied, and its kinetics have been evaluated in a composite form as

$$\text{rate} = k_0[IO_3^-][S][H^+]^2 \qquad (1)$$

where S is any 2-electron reductant. If S is iodide, then the rate-limiting step can be written as[30]

$$IO_3^- + 2H^+ + I^- \rightarrow HIO_2 + HOI \qquad (R9)$$

$HIO_2$ and HOI represent the active oxyiodine species that perform the bulk of the subsequent oxidations. Iodate itself is relatively inert. Thus any induction period observed denotes the time taken for the buildup of the reactive species. Iodate solutions always contain at least $10^{-6}$ M of iodide ions, and these are normally sufficient to initiate the reaction because only catalytic amounts are needed. The rest of the iodide ions are produced as the reaction proceeds. Further reaction of HOI, for example, immediately produces $I^-$, which can be recycled and used in reaction R9:

$$HOI + GTU \rightarrow GTU\text{-}C + H_2O + H^+ + I^- \qquad k_{10} \quad (R10)$$

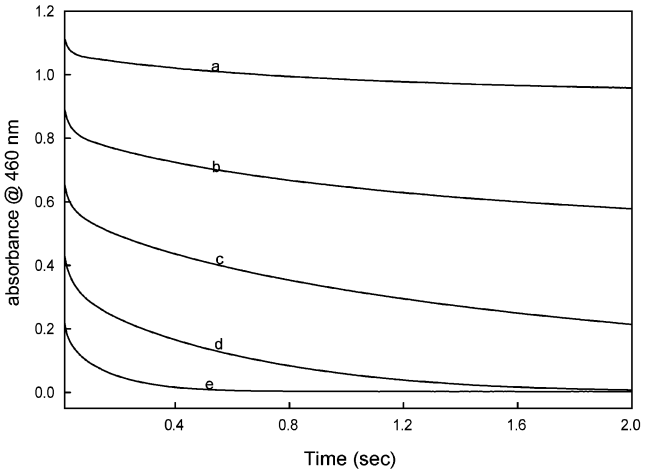


**Figure 7.** Effect of GTU variation on its oxidation by $I_2/I_3^-$ solutions. There is faster initial consumption of iodine followed by a rapid shutdown of the reaction as it proceeds. $[I_2]_o = 0.0015$ M, $[GTU]_o$ = (a) 0.0005, (b) 0.001, (c) 0.0015, (d) 0.002, (e) 0.0025 M.

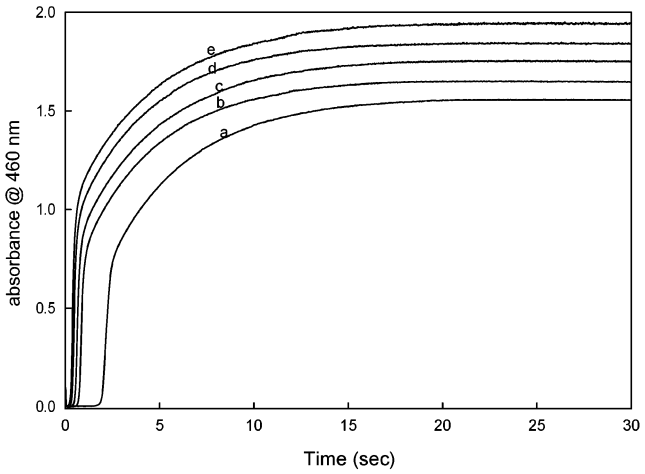


**Figure 8.** $[I^-]_o$ effect on the iodate oxidation of GTU. The effect of iodide can be seen on the reduced induction period and increased final absorbance of iodine as iodide concentration is increased. $[GTU]_o$ = 0.01 M, $[H^+]_o = 0.02$ M, $[IO_3^-]_o = 0.01$ M, $[I^-]_o$ = (a) no iodide, (b) 0.00025, (c) 0.0005, (d) 0.00075, (e) 0.001 M.

$HIO_2$ can also disproportionate in the presence of iodide to produce more HOI:

$$HIO_2 + I^- + H^+ \rightleftharpoons 2HOI \qquad (R11)$$

Reactions R9 and R11 have been extensively studied,[31] and their kinetics parameters are known.

**Iodine Formation.** There is a single reaction that can be identified in this reaction network as being responsible for the formation of iodine. It is the reverse of the iodine hydrolysis reaction:[32]

$$HOI + I^- + H^+ \rightleftharpoons I_2(aq) + H_2O \qquad K_H^{-1} \quad (R12)$$

This reaction has to compete with the other reactions that consume iodine. The predominant route to consumption of iodine is the direct reaction of iodine with the substrate:

$$I_2 + GTU \rightarrow GTU\text{-}C + 2I^- + 2H^+ \qquad (R13)$$

Figure 5b shows that this reaction is autoinhibitory, but as long as there is a sink for iodide, which, in this case, is made up of

reactions R11 and R12, autoinhibition will not asset itself. Visible formation of iodine, which denotes the end of the induction period occurs when reaction R12 exceeds reaction R13:

$$\frac{d[I_2]}{dt} = V_{12} - V_{13} \tag{2}$$

These reactions are effectively buffered because acid concentrations far exceed the concentrations of the reacting species. Reaction R12 will depend on the rate of formation of HOI in reaction R9, hence the indication, in Figure 2b, that the overall reaction is controlled by acid to the second power.

**Iodine Consumption.** Figures 5a and 7 suggest that the reaction of iodine with GTU is first order in both iodine and GTU. The initial step in this reaction is an electrophilic attack on the sulfur center of GTU by iodine:

$$I_2 + >C{=}S \rightleftharpoons [>C{=}S{-}I]^+ + I^- \tag{R14}$$

This is then followed by a hydrolysis:

$$[>C{=}S{-}I]^+ + H_2O \rightarrow >C{-}SOH + I^- + 2H^+ \tag{R15}$$

$>C-SOH$ represents the transient sulfenic acid that is formed before the ring cyclization occurs to form 3,5-diamino-1,2,4-thiadiazole:

$$>C{-}SOH \rightarrow \text{GTU-C} + H_2O \tag{R16}$$

Iodide inhibition would suggest that the triiodide species is inert toward GTU or at least is a poorer electrophile. If one considers it inert, then the rate of iodine consumption will be given by

$$\frac{-d[I_2]}{dt} = \frac{k_{13}[\text{GTU}][I_2]_0}{1 + K_{eq}[I^-]} \tag{3}$$

where $[I_2]_0$ is the initial concentration of iodine. Because $K_{eq}$, at 770 $M^{-1}$, is high, small amounts of iodide can induce a visible retardation. Equation 3 supports the data shown in Figure 5b, which predicts a saturation as iodide concentrations are increased.

**Acid Dependence.** Acid retardation is difficult to rationalize because there are two reasonable ways in which acid could effect a retardation of the oxidation of GTU by iodine. The first possibility is through the deactivation of the sulfur center for electrophilic attack by acid:

$$>C{=}S + H^+ \rightarrow [>C{=}S{-}H]^+ \qquad K_a^{-1} \tag{R17}$$

This protonation should be rapid in both directions, but it effectively blocks reaction R14, which represents the electron transfer from the sulfur center to iodine. Incorporating the retardation by acid into the overall rate of reaction gives the following rate equation:

$$\frac{-d[I_2]}{dt} = \frac{k_{13}[\text{GTU}]_0[I_2]_0}{(1 + K_{eq}[I^-])(1 + K_a^{-1}[H^+])} \tag{4}$$

Equation 4 supports the data shown in Figure 6a,b.

The other kinetically indistinguishable way in which acid could effect a retardation is through the hydrolysis reaction R12. High acid would deplete hypoiodous acid, HOI, in favor of molecular iodine. If HOI is a faster oxidizing agent that $I_2$, then an increase in acid would decrease the rate of reaction. In this case, both $I_2$ and HOI are active, and a plot of inverse acid concentrations versus initial rate should show a straight line with a positive intercept (see Figure 6b). The rate of consumption of iodine can then be derived as

$$\frac{-d[I_2]}{dt} = [\text{GTU}](k_{10}[\text{HOI}] + k_{13}[I_2]) \tag{5}$$

After elimination of HOI, the rate equation can be deduced to be

$$\frac{-d[I_2]}{dt} = [\text{GTU}][I_2]\left(k_{13} + \frac{k'}{[H^+][I^-]}\right) \tag{6}$$

where $k' = K_H \bullet k_{10}$

Using the mass balance equation on the iodine species of

$$2[I_2]_0 = 2[I_2] + [\text{HOI}] + [I^-] \tag{7}$$

one can rewrite eq 6 as

$$\frac{-d[I_2]}{dt} = [\text{GTU}][I_2]_0 \frac{\left\{k_{13} + \frac{k'}{[H^+][I^-]}\right\}}{\left\{1 + \frac{K_H}{[H^+][I^-]}\right\}} \tag{8}$$

Equation 8 combines oxidation pathways R10 and R13. This equation can be simulated to anticipate the functional dependence of the rate of reaction with respect to acid, iodide, oxidant, and reductant. Burger and Liebhafsky[33] evaluated $K_H$ as $4.13 \times 10^{-12}$ $M^2$, and substituting this value into eq 8 predicts acid dependence for pH conditions above 9 and virtually no acid effects below this pH because at low pH conditions, $1 \gg K_H/[H^+][I^-]$. This is contrary to our observations. We can conclude that eq 4 represents the correct rate law in our mechanism and that at fixed iodide concentrations, reasonable acid retardation will be observed within the pH range used in this study and the same applies to the iodide inhibition. Equation 4 is derived from the assumption that both the triiodide complex and the protonated GTU are inert, or at least react much more sluggishly than uncomplexed iodine and unprotonated GTU. The equilibria for the formation of these inert forms are rapid in both directions.

**Evaluation of Rate Constants.** If we assume constant acid concentrations, we can rewrite eq 3 in terms of iodide concentrations as a function of $K_{eq}$ and initial rate of the reaction:

$$[I^-] = \left(\frac{k_{13}}{K_{eq}}\right)\left(\frac{[\text{GTU}]_0[I_2]_0}{\text{mod}|\text{rate}|}\right) - \frac{1}{K_{eq}} \tag{9}$$

where mod|rate| is the initial rate of the reaction expressed as $-d[I_2]/dt$. Equation 9 is also valid in unbuffered reaction solutions at initial conditions. A plot of the initial iodide concentrations vs the inverse of the initial rate should give a straight line with intercept $K_{eq}^{-1}$. This plot is shown as Figure 5d. This plot was first performed without weighting factors in an effort to see how close to the literature value of $K_{eq}$ these series of experiments would deliver. This analysis gave $K_{eq} = 440 \pm 40$ $M^{-1}$. Later the intercept was weighted at the inverse of the expected value of 770 $M^{-1}$ and treatment based on eq 9 gave a value of $k_{13} = (1.10 \pm 0.2) \times 10^4$ $M^{-1}$ $s^{-1}$. The same treatment was extended to acid dependence experiments (Figure 6a,b) to evaluate a reasonable value for $K_a^{-1}$. We could equally

**TABLE 1: Mechanism of the Iodate−Guanylthiourea Reaction**

| rxn no. | reaction | $k_f$; $k_r$ |
|---|---|---|
| M1 | $IO_3^- + GTU + H^+ \rightarrow GTU{-}C + HIO_2$ | 80 |
| M2 | $HIO_2 + I^- + H^+ \rightleftharpoons 2HOI$ | $2.1 \times 10^9$, 90 |
| M3 | $IO_3^- + HOI + H^+ \rightleftharpoons 2HIO_2$ | $8.6 \times 10^2$, 2.0 |
| M4 | $HOI + I^- + H^+ \rightleftharpoons I_2(aq) + H_2O$ | $3.1 \times 10^{12}$, 2.2 |
| M5 | $IO_3^- + 2H^+ + I^- \rightleftharpoons HIO_2 + HOI$ | 2.8, $1.44 \times 10^3$ |
| M6 | $I_2(aq) + I^- \rightleftharpoons I_3^-(aq)$ | $6.2 \times 10^9$, $8.5 \times 10^6$ |
| M7 | $I_2 + GTU \rightarrow GTU{-}C + 2I^- + 2H^+$ | $1.1 \times 10^4$ |
| M8 | $HOI + GTU \rightarrow GTU{-}C + H_2O + H^+ + I^-$ | $7.5 \times 10^3$ |
| M9 | $GTU + H^+ \rightleftharpoons [GTU{-}H]^+$ | $5.0 \times 10^6$, $5.6 \times 10^3$ |

[a] Legend: GTU, guanylthiourea; GTU-C, 3,5-diamino-1,2,4-thiadiazole.

rearrange eq 4 after assuming constant iodide ($3.36 \times 10^{-4}$ M in this set of experiments):

$$[H^+] = \left(\frac{k_{13}}{K_a^{-1}}\right)\left(\frac{[GTU]_0[I_2]_0}{\text{mod}|\text{rate}|}\right) - \frac{1}{K_a^{-1}} \qquad (10)$$

where, in this case, $k_{13} = k_{13}(1 + K_{eq}[I^-])^{-1}$, which gave a numerical value of $0.795k_{13}$ for the data shown in Figure 6b. Using the value of $k_{13}$ evaluated in eq 9 and data treatment shown in Figure 5d, from the slope of the graph in Figure 6b we managed to evaluate a value of $K_a^{-1} = (8.9 \pm 1.3) \times 10^2$ $M^{-1}$, which is related to the $K_b$ of the thiocarbonyl group in GTU. Using only the intercept value of eq 10 gave a slightly higher value of $K_a^{-1}$, $(9.8 \pm 2.2) \times 10^2$ $M^{-1}$. The value of $K_a^{-1}$ derived from the slope, however, delivers a more accurate value for $K_a^{-1}$ because the intercept amplifies the errors generated in the slope.

**Overall Mechanism.** The overall reaction mechanism can be summarized in the form of Table 1. It is a simple reaction scheme made up of nine reactions distilled from all the possible reactions. The mechanism is dominated by four well-known oxyiodine reactions (M2−M5),[24,25,34,35] one rapid $I_2/I^-$ equilibrium (M6),[29,36] one protolytic reaction (M9), and three irreversible oxyiodine−GTU reactions (M1, M7, and M8). This simple mechanism is able to explain and reproduce the complex oligooscillatory behavior observed in this reaction system. The rapid reaction M2[28] can allow us to ignore any reactions that involved intermediate iodous acid, $HIO_2$, as an oxidant. Reaction M1 is the initiation step, together with M5. Only trace amounts of iodide are needed to initiate the reaction because as the reaction proceeds, there is autocatalytic production of iodide. This is evident from the composite reaction M1 + M2:

$$IO_3^- + GTU + 2H^+ + I^- \rightarrow GTU\text{-}C + 2HOI + H_2O \quad (R18)$$

when one combines reaction R18 with the faster oxidation of GTU by HOI (reaction M8), then the overall process (M1 + M2 + M8) shows that one iodide ion will produce 2 iodide ions as in typical quadratic autocatalysis.

$$IO_3^- + 3GTU + I^- \rightarrow 3GTU\text{-}C + 2I^- + 3H_2O \quad (R19)$$

The addition of small amounts of iodide (see Figure 8) will catalyze the reaction by instantly making reaction R9 viable from $t = 0$ without having to build up the concentration of iodide from stoichiometry R19. However, this catalytic effect quickly attains a saturation as in excess iodide, reaction R9 will still remain the rate-determining step with a standard squared dependence on acid. Figure 8 also shows the diminished catalytic abilities of iodide as it is steadily increased. The observation of exotic dynamics, as in this reaction, needs nonlinear kinetics in the form of either autocatalysis, autoinhibition (reactions M6 and M9), or a combination of both as is the case in this reaction.

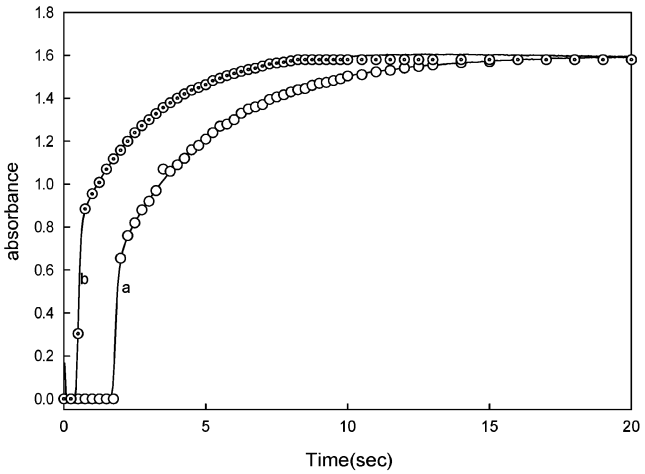


**Figure 9.** Computer modeling: Traces showing the simulated results (circles) and the experimental data (solid line) for data shown in Figure 3a. $[GTU] = 1 \times 10^{-2}$ M; $[IO_3^-] = 3 \times 10^{-2}$ M; trace (a) $[H^+] = 0.015$ M; trace (b) $[H^+] = 0.02$ M.

**Computer Simulations.** The simple mechanism in Table 1 was simulated using fourth-order Runge−Kutta techniques derived from the *Chemical Kinetics Simulator* from IBM's Almaden group. Five of the nine reactions (M2−M6)[23−25,30,37] have kinetics parameters well-documented in literature, and this work derived the rate constants for one of the reactions (M7). Reaction M8 could be estimated from M7 and this left only two reactions that could be adjusted for best fit: M1 and M9. Because we managed to derive some reasonable value for $K_a^{-1}$, this meant that after guessing a value for $k_{M9}$, the reverse was fixed by the equilibrium constant. Reaction M1 became less important in conditions where small amounts of iodide were added prior to start of the reaction (Figure 8). Under these conditions, reaction control was simply based on reaction M5. Our removal of $HIO_2$ as an active oxidant meant that reaction M2 became very important and the global reaction dynamics were very sensitive to the kinetics parameters of M2; even though literature values are available. For most of our simulations, we used $k_{-M2}$ of $1.20 \times 10^2$ $M^{-1}$ $s^{-1}$, despite the fact that a value of 90 $M^{-1}$ $s^{-1}$ is the suggested literature value. Reaction M6 is known, through laser Raman temperature-jump experiments[29] to be rapid in both directions. However, the use of these literature values rendered the simulations extremely stiff, requiring over 12 h on a Pentium IV 2.4 GHz computer to simulate a typical result shown in Figure 8. Reduction of the forward and reverse rate constants by a factor of 100 sped up the simulations without altering the predicted trajectories. Thus, for most of our simulations, values of $k_{M6} = 6.2 \times 10^7$ $M^{-1}$ $s^{-1}$ and $k_{-M6} = 8.5 \times 10^4$ $s^{-1}$ were used. Despite the simplicity of the mechanism, it was still able to simulate all the observed global dynamics of the reaction except some qualitative aspects of the data shown in Figure 4b. Though the mechanism could simulate the peak concentrations of iodine and their (period of) occurrence, it produced peaks that were much sharper than those that were experimentally observed. However, the mechanism was able to satisfactorily model data in Figures 2a, 3a, 5a−c, 6a, 7, and 8. Figure 9 shows a simulations fit to the data in Figure 3a (traces a and e). There is a very reasonable fit to the experimentally observed induction period, rate of formation of iodine, the total amount of iodine formed and the acid dependence. The iodide dependence experiments shown in

Figure 5c were the easiest to simulate because we could shut down all the reactions in the mechanism except reactions M6−M8, with the only tunable parameter being $k_{M7}$. This also helped in establishing our experimental value for $k_{M7}$.

**Acknowledgment.** This work was supported by Grant Number CHE 0137435 from the National Science Foundation.

## References and Notes

(1) Part 8 (of 10) in the series of publications to honor the memory of Dr. Cordelia R. Chinake (1965−1998). Part 7. Oxyhalogen−Sulfur Chemistry: Kinetics and Mechanism of Oxidation of *N*-acetylthiourea by chlorite. Submitted for publication to *Int. J. Chem. Kinet*.

(2) Saillenfait, A. M.; Sabate, J. P.; Langonne, I.; de Ceaurriz, J. *Fundam. Appl. Toxicol.* **1991**, *17*, 399−408.

(3) Boyd, M. R.; Neal, R. A. *Drug Metab. Dispos.* **1976**, *4*, 314−322.

(4) Ulland, B. M.; Weisburger, J. H.; Weisburger, E. K.; Rice, J. M.; Cypher, R. *J. Natl. Cancer Inst.* **1972**, *49*, 583−584.

(5) Ziegler-Skylakakis, K.; Nill, S.; Pan, J. F.; Andrae, U. *Environ. Mol. Mutagen.* **1998**, *31*, 362−373.

(6) Svarovsky, S. A.; Simoyi, R. H.; Makarov, S. V. *J. Phys. Chem. B* **2001**, *105*, 12634−12643.

(7) Araujo, M. C.; Antunes, L. M.; Takahashi, C. S. *Teratog. Carcinog. Mutagen.* **2001**, *21*, 175−180.

(8) Poulsen, L. L.; Hyslop, R. M.; Ziegler, D. M. *Arch. Biochem. Biophys.* **1979**, *198*, 78−88.

(9) Jonnalagadda, S. B.; Chinake, C. R.; Simoyi, R. H. *J. Phys. Chem.* **1996**, *100*, 13521−13530.

(10) Busser, M. T.; Lutz, W. K. *Carcinogenesis* **1987**, *8*, 1433−1437.

(11) Stevens, G. J.; Hitchcock, K.; Wang, Y. K.; Coppola, G. M.; Versace, R. W.; Chin, J. A.; Shapiro, M.; Suwanrumpha, S.; Mangold, B. L. *Chem. Res. Toxicol.* **1997**, *10*, 733−741.

(12) Decker, C. J.; Doerge, D. R.; Cashman, J. R. *Chem. Res. Toxicol.* **1992**, *5*, 726−733.

(13) Scott, A. M.; Powell, G. M.; Upshall, D. G.; Curtis, C. G. *Environ. Health Perspect.* **1990**, *85*, 43−50.

(14) Mohr, H. J.; Nothdurft, H. *Int. Arch. Arbeitsmed.* **1967**, *23*, 168−174.

(15) Kim, S. G.; Kim, H. J.; Yang, C. H. *Chem. Biol. Interact.* **1999**, *117*, 117−134.

(16) Svarovsky, S. A.; Simoyi, R. H.; Makarov, S. V. *J. Chem. Soc., Dalton Trans.* **2000**, 511−514.

(17) Makarov, S. V.; Mundoma, C.; Svarovsky, S. A.; Shi, X.; Gannett, P. M.; Simoyi, R. H. *Arch. Biochem. Biophys.* **1999**, *367*, 289−296.

(18) Timofeev, N. N.; Frolov, S. F.; Zhitniuk, R. I. *Vestn. Khir. Im I. I. Grek.* **1975**, *115*, 39−43.

(19) Vertesi, C. *Med. Hypotheses* **1993**, *40*, 335−341.

(20) Gergely, P.; Lang, I.; Gonzalez-Cabello, R.; Feher, J. *Tokai J. Exp. Clin. Med.* **1986**, *11 Suppl*, 207−213.

(21) Wainson, A. A.; Uriupov, O. I. *Radiobiologiia* **1986**, *26*, 329−333.

(22) Jonnalagadda, S. B.; Chinake, C. R.; Olojo, R.; Simoyi, R. H. *Int. J. Chem. Kin.* **2002**, *34*, 237−247.

(23) Kolaranic, L.; Schmitz, G. *J. Chem. Soc., Faraday Trans.* **1992**, *88*, 2343−2349.

(24) Schmitz, G. *Phys. Chem. Chem. Phys.* **2000**, *2*, 4041−4044.

(25) Schmitz, G. *Phys. Chem. Chem. Phys.* **1999**, *1*, 1909−1914.

(26) Rabai, G.; Beck, M. T. *J. Chem. Soc., Dalton Trans.* **1985**, 1669−1672.

(27) Chinake, C. R.; Mambo, E.; Simoyi, R. H. *J. Phys. Chem.* **1994**, *98*, 2908−2916.

(28) Xie, Y.; McDonald, M. R.; Margerum, D. W. *Inorg. Chem.* **1999**, *38*, 3938.

(29) Turner, D. H.; Flynn, G. W.; Sutin, N.; Beitz, J. V. *J. Am. Chem. Soc.* **1972**, *94*, 1554−1559.

(30) Liebhafsky, H. A.; Roe, G. M. *Int. J. Chem. Kinet.* **1971**, *11*, 693−701.

(31) Agreda, J. A.; Field, R. J.; Lyons, N. J. *J. Phys. Chem. A* **2000**, *104*, 5269−5274.

(32) Kustin, K., Eigen, M. *J. Am. Chem. Soc.* **1962**, *84*, 1355−1359.

(33) Burger, J. D.; Liebhafsky, H. A. *Anal. Chem.* **1973**, *45*, 600−602.

(34) Lalitha, P. V. N.; Ramaswamy, R. *Collect. Czech. Chem. Commun.* **1992**, *57*, 2235−2240.

(35) Tiktonova, L. P.; Kovalenko, A. S.; Labunskaya, I. F.; Ivashchenko, T. S. *Teor. Eksp. Khim.* **1991**, *27*, 737−741.

(36) Ruasse, M.-F.; Aubard, J.; Galland, B.; Adenir, A. *J. Phys. Chem.* **1986**, *90*, 4382−4388.

(37) Urbansky, E. T.; Cooper, B. T.; Margerum, D. W. *Inorg. Chem.* **1997**, *36*, 1338−1344.